

Thermodynamic Properties of Electrons in Small Metal Particles*

R. Denton[†] and B. Mühlischlegel[‡]

Institut für Theoretische Physik, Universität zu Köln, Köln, Germany

D. J. Scalapino[†]

University of California, Santa Barbara, California 93106

(Received 9 October 1972)

The electronic properties of an assembly of small metal particles are determined by and reflect their distribution of discrete electronic energy levels. With the absence of strong correlations (arising from, for example, the presence of localized impurities or surface states), it is reasonable to treat the energy-level distribution statistically. The level distribution is determined by the symmetry of the dynamics which governs the three ensembles of the statistical theory of spectra and characterized by a mean single-electron-level spacing δ for particles of a certain size. In this paper we confine our attention to the thermodynamics of small particles. The exact solution of a model is presented which consists of electrons in equally spaced levels and which includes magnetic field and short-range-interaction effects. We report on detailed calculations of the heat capacity and magnetic spin susceptibility. Here, the statistics of level distributions is applied in the whole temperature range, thus generalizing the work done originally by Kubo and Gor'kov and Eliashberg for the limiting case in which $kT \ll \delta$.

I. INTRODUCTION

The purpose of this paper is to consider in detail the static electronic properties of a collection of small metallic particles. In treating the bulk electronic properties of metals, one usually considers the thermodynamic limit in which the particle number and volume go to infinity with the density N/V finite. In this case, the single-particle energy levels form a continuum. However, for finite systems at sufficiently low temperatures the discrete nature of the single-particle spectrum can be expected to enter. For a finite system, the average spacing δ between single-electron states is of order ϵ_F/N , where ϵ_F is the Fermi energy and N is the number of conduction electrons. If kT is of order or less than δ , then the discrete character of the spectrum will affect the static thermal properties such as heat capacity and magnetic susceptibility. As kT becomes large compared to δ , many levels enter in determining the thermodynamic properties and the discrete effects are washed out.

The single-particle spectrum will appear discrete so long as the level width Γ is less than the spacing δ . Using the bulk low-temperature limit as an estimate,

$$\Gamma \sim (kT)^2 / \epsilon_F,$$

and the condition for the spectrum to be discrete becomes

$$N < (\epsilon_F / kT)^2.$$

This is of course satisfied when $\delta > kT$. However, even when $kT \gg \delta$, N can be such that the basic

level structure is discrete. In this case, although the static thermodynamic properties will not reflect the underlying discrete nature of the single-particle spectrum, it should still be possible to probe it dynamically. Here we consider only the thermodynamic problem and restrict our analysis to the static electronic properties.¹

Our basic assumptions about a single small metal particle and about a collection of such particles will be similar to the work of Kubo.² In this context we want to draw attention to a very readable short review on small metal particles written by the same author.³ In that work the justification for using a noninteracting quasiparticle scheme at low temperatures was indicated. The quasiparticles take into account the main effects of the electron-electron and electron-phonon interactions and are described by the single-spin density of states $N(0)$. This density of states varies negligibly over the energy range one needs to consider, which involves a relatively small number of levels about the Fermi level. The average level spacing δ is given by the inverse of the single-spin density of states $1/N(0)$. Since the density of states is proportional to the volume of the particle, δ then varies as the inverse of the volume. A metallic particle of size a of order 100 \AA , containing about 10^5 conduction electrons, would correspond to a level separation $\delta/k \sim 1 \text{ K}$. To calculate properties of small particles at this low temperature, one needs to consider all quasiparticle excitations for levels near the Fermi surface, with the enumeration of the states consistent with the Pauli principle.

Kubo recognized the electrostatic energy associated with the addition or removal of an electron

from a small particle is extremely large compared to the thermal energy available; the ratio of the two is approximately given by $e^2/a\delta$ which is of order 10^3 for a particle 100 \AA in size. Thus if the grand canonical ensemble is used, this interaction must be included. Alternatively, the number N of electrons in a particle can be treated as a constant so that the canonical ensemble becomes appropriate for this problem. We will examine the case of equal level spacings which can be exactly solved and allows a comparison of the canonical and grand canonical solutions for the specific heat and susceptibility. In addition, the exact solution displays a periodicity in the magnetic field which is a characteristic feature of the equal level system.

Another feature of small particles at low temperatures is the difference in behavior between particles with an even and odd number of conduction electrons. This effect in the susceptibility was first noted by Greenwood, Brout, and Krumhansl.⁴ At low temperatures such that only a few levels are involved, the exact counting of the possible excitations for the even and odd cases leads to this difference. In the grand canonical ensemble the difference results from the positioning of the chemical potential in the Fermi distribution. For a measurement such as the specific heat for which one cannot distinguish between the even and odd particles in the collection, one can take a simple average assuming equal numbers of each type. For Knight-shift measurements, the frequency separation of nuclear resonances in particles with even and odd numbers of electrons may allow one to study these as two distinct species. The even-odd effects wash out as kT becomes of order δ .

Let us consider a collection of isolated small particles all of the same size. The distribution of electronic energy levels in these particles may contain strong correlations arising, for example, from the presence of localized impurities or surface states. In the present work we assume that such correlations are absent. For this case Kubo² has emphasized that the originally degenerate energy levels calculated for a regular object such as a sphere are in reality split apart by atomic irregularities on the surface; the resulting nondegenerate spectrum has an average level spacing δ of order $\delta = \epsilon_F/N$. The level spectrum of two particles will then be different due to uncontrollable surface irregularities but will have the same average spacing δ . Now for a given particle the one-electron matrix elements arising from surface perturbations can still contain minor correlations. However, experimentally one deals with an ensemble of particles, for which the surface perturbations of one particle are uncorrelated with those of another. For the purpose of calculating the energy-

level distribution for an ensemble of particles, we feel it is a reasonable approximation to treat the matrix elements as "randomly" distributed independently of the others. The influence of the perturbation matrix elements in determining the level distribution is then susceptible to a statistical treatment, and only a knowledge of the symmetries of the Hamiltonian is necessary to determine the level distribution for the ensemble of particles. The statistical description of the energy-level distribution has been developed by Wigner,⁵ Dyson,⁶ Metha,⁷ Porter⁸ and others. The effect of the various statistical level distributions on the static properties of the collection of small particles will be calculated. The measurements of specific heat and susceptibility could test the validity of the theoretical considerations leading to the statistical distributions, such as the assumed lack of significant correlation among the matrix elements.

The paper is divided as follows: Sec. II contains a discussion of the statistical description of energy levels and its applicability to a collection of small particles. Section III presents the exact solution to the equal-level problem. The first derivation is obtained by projecting the canonical partition function from the grand canonical expression. The second derivation involving the Tomonaga model is generalized to include a simple short-range ferromagnetic interaction. A comparison between the canonical and grand canonical results is made, and the periodic features characteristic of equal levels are also displayed. Section IV applies the statistical description of energy levels to calculate the specific heat and spin susceptibility. The folding of the results into a particle size distribution is also discussed.

II. DISTRIBUTION OF ENERGY LEVELS

To calculate the thermodynamics of a collection of small metal particles at low temperatures, one needs the distribution of energy levels about the Fermi level. Since very general theoretical assumptions have led to a number of statistical ensembles for the distribution of energy levels, we discuss their applicability to small particles in this section.

The essential features in the statistical treatment first appeared in the level distribution studies of complex nuclear and atomic systems.⁸ Wigner⁵ considered the possibility of describing the levels of a complex nuclear system statistically as the eigenvalues of a random matrix. The Hamiltonian H_{ij} of a single nuclear system is represented by a matrix for some set of basis states, and in turn an ensemble of matrices would correspond to an ensemble of possible nuclear systems. The elements in the matrices would be random in the restricted sense that the individual matrices must still satisfy

the properties imposed by the symmetries which the individual Hamiltonians are assumed to have in common. The possible ensembles of random $n \times n$ matrices, corresponding to various symmetry requirements, can then be diagonalized to yield the respective distributions of ordered energy eigenvalues.

Now a single small particle has a well-defined set of energy levels, which one could in principle calculate. In the familiar case of a perfect metallic sphere, the distribution of energy levels is not difficult to obtain; the degeneracy in magnetic quantum numbers due to the spherical symmetry is proportional to $N^{1/3}$, where N is the number of conduction electrons. However, atomic irregularities on the surface are sufficient to split apart this large degeneracy of energy levels. For a 100-Å particle the wave numbers of interest are of order 1 \AA^{-1} . Thus in practice it would be extremely difficult to calculate the actual distribution of energy levels, due to the many small perturbations on the surface.

On the other hand, just as for the nuclear system, the Hamiltonians for the collection of small particles can be represented by an ensemble of matrices. The actual distributions of energy levels for the entire collection could be described by a statistical distribution of one-electron levels, obtained from diagonalizing the matrices. One would expect the off-diagonal elements in each matrix arising from the surface irregularities not to be highly correlated with one another, except in the case of actually conserved quantum numbers. With no spin-orbit coupling, for example, the electron spin is a good quantum number and there would be no matrix elements between opposite-spin states. The energy-level degeneracy would then be split apart except for the remaining twofold spin degeneracy. Even if there is some correlation of the matrix elements for a single small particle, the irregularities on the surface of an assembly of small particles vary from one particle to another. Thus we feel it is reasonable to apply the general theory of statistical ensembles, which is based on random matrix elements, to the problem of small metal particles.

In general, the Hamiltonian matrix has symmetric-real, quaternion-real, or complex elements. Dyson has shown in his fundamental work that these symmetries are completely classified in terms of the orthogonal, symplectic, and unitary groups, respectively. Each group uniquely defines an ensemble, and we summarize their applicability below. The orthogonal ensemble, which has already been applied to nuclear and atomic systems,⁸ corresponds to systems with (a) time-reversal invariance and (b) integral values of angular momentum, or rotational invariance in the case of angular momentum with

half-integral values. In the limiting case of no spin-orbit coupling in a small particle, the spin is a conserved quantum number. Therefore, only the orbital parts of the one-electron states mix together due to the irregularities on the surface. The relevant angular momentum is the orbital angular momentum which is, of course, integral, so that in the absence of a magnetic field condition, (b) is satisfied and the orthogonal ensemble is applicable. The symplectic ensemble applies to systems with (a) time-reversal invariance and (b) half-integral values of angular momentum, with no rotational invariance. If the spin-orbit coupling becomes strong enough to completely mix the levels which would have been determined according to the orthogonal ensemble previously, then the symplectic ensemble is appropriate to determine the level distribution. For a rough measure of the spin-orbit coupling strength of the metallic particle one can use the appropriate atomic spin-orbit coupling λ . The symplectic ensemble is applicable when the ratio λ/δ becomes of order 1. For δ of order 1 K the symplectic ensemble would be appropriate for all but the lightest metals. Finally, the unitary ensemble corresponds to particles with spin-orbit coupling and no time-reversal invariance. In this case the magnetic field must be strong enough to further mix the levels together so that the symplectic ensemble no longer applies. This should occur when $\frac{1}{2}g\mu_B H$ becomes of order δ , where g is the Landé g factor of the electrons. The above conditions fairly well specify the applicability of each ensemble. However the actual details of the transition from one ensemble to another, in going from one material to another or in turning on the magnetic field, have not been examined comprehensively.

The normalized distributions of N ordered eigenvalues for the three ensembles, obtained by diagonalizing the matrices in each ensemble, are given by⁶

$$W_N^{(\gamma)}(\epsilon_1, \dots, \epsilon_N) = C_N^{(\gamma)} \exp\left(-\frac{\gamma}{2} \sum_i \epsilon_i^2\right) \prod_{j < k} |\epsilon_j - \epsilon_k|^\gamma, \quad (1)$$

where $C_N^{(\gamma)}$ is chosen to give the normalization

$$\int_{-\infty}^{\infty} \dots \int W_N^{(\gamma)}(\epsilon_1, \epsilon_2, \dots, \epsilon_N) d\epsilon_1 d\epsilon_2 \dots d\epsilon_N = 1. \quad (2)$$

Here γ takes on the values 1, 2, and 4 for the orthogonal, unitary, and symplectic ensembles, respectively. Each pair of eigenvalues in the formula above displays a level "repulsion," which in the case of the orthogonal ensemble goes as the first power as the two eigenvalues approach one another. To the other ensembles correspond different power laws, due to the different symmetries satisfied by their Hamiltonians. The repulsion expresses the fact that an accidental degeneracy is

very unlikely; the perturbations represented by the off-diagonal elements in the random matrices will split apart any eigenvalues which approach one another.

The physical properties of small particles depend upon the distribution of eigenvalues near the Fermi level. In general, the Fermi level will have many levels lying both above and below it. Therefore, the eigenvalue distribution near the Fermi level can be obtained from the limiting behavior of $W_N^{(n)}$, for large N , by integrating over all but a few of the eigenvalues in the middle of the spectrum.

$$P_{n-1}^{(n)}(\epsilon_i, \dots, \epsilon_{i+n}) \\ = \lim_{N \rightarrow \infty} \int W_N^{(n)}(\epsilon_1, \dots, \epsilon_N) d\epsilon_1 \dots d\epsilon_{i-1} d\epsilon_{i+n+1} \dots d\epsilon_N.$$

Near the center of the eigenvalue spectrum, the absolute level position is irrelevant and $P_{n-1}^{(n)}$ is a function of the n level spacings $\Delta_1 = \epsilon_{i+1} - \epsilon_i$, $\Delta_2 = \epsilon_{i+2} - \epsilon_{i+1}$, ..., $\Delta_n = \epsilon_{i+n} - \epsilon_{i+n-1}$. The subscript $n-1$ denotes the number of levels between the two outermost levels. Thus $P_0^{(n)}(\Delta)$ represents the probability that two levels are separated by an energy Δ ; $P_1^{(n)}(\Delta_1, \Delta_2)$ the probability that three levels have the relative spacings Δ_1 and Δ_2 ; etc.

For the nearest-neighbor spacing distributions $P_0^{(n)}(\Delta)$, exact numerical results as well as various asymptotic forms are known.⁸ In the limit where Δ is small compared to the average level spacing δ , the orthogonal, unitary, and symplectic distributions vanish as various powers of Δ/δ reflecting the level repulsion effects:

$$P_0^{(1)}(\Delta) = \frac{\pi^2}{6} \frac{\Delta}{\delta^2}, \quad P_0^{(2)}(\Delta) = \frac{\pi^2}{3} \left(\frac{\Delta}{\delta}\right)^2 \frac{1}{\delta}, \\ P_0^{(4)}(\Delta) = \frac{32}{270} \pi^4 \left(\frac{\Delta}{\delta}\right)^4 \frac{1}{\delta}. \quad (3)$$

Numerical results over the entire Δ/δ range are known for $P_0^{(n)}$. However, for larger numbers of levels, exact results for the $P_{n-1}^{(n)}$ distributions become increasingly difficult to determine, and various approximate schemes have been devised.⁸

It is necessary for the calculations later to obtain simple approximations to the exact formulas. As has been noted by others,⁸ useful approximations to the exact nearest-neighbor spacing distributions $P_0^{(n)}$ are obtained by taking $N=2$ in Eq. (1), changing variables to the spacing between the two eigenvalues, and integrating over the remaining variable. For example, using the orthogonal ensemble this procedure yields the "Wigner surmise":

$$P_W(\Delta) = \frac{\pi}{2} \frac{\Delta}{\delta^2} e^{-\pi(\Delta/\delta)^2/4}. \quad (4)$$

This normalized distribution function was proposed by Wigner to fit the nuclear data for the spacing

between two adjacent eigenvalues. The close agreement between $P_0^{(1)}(\Delta)$, given in Eq. (3), and the approximate $P_W(\Delta)$ has been noted before.^{6,9} In the Appendix, we generalize this procedure to obtain approximate formulas for the more complicated distributions.

We mention also the Poisson or "random" distribution, which was first applied by Kubo.² If the irregular potential for the small particles merely had diagonal matrix elements among the crystal states, this uncorrelated or random distribution would be appropriate. In this case, the nearest-neighbor spacing goes as

$$P_0(\Delta) = e^{-\Delta/\delta}. \quad (5)$$

There is no level repulsion since there are no off-diagonal elements to cause the level separation. Because of the neglect of the off-diagonal elements, this distribution is unphysical, and we will use it simply for comparison. Note that while the random nearest-neighbor distribution, Eq. (5), approaches the bulk density of states δ^{-1} as $\Delta/\delta \rightarrow 0$, the $P_0^{(n)}$ distributions, Eq. (3), vanish as $(\Delta/\delta)^n$. This difference has a profound influence on the low-temperature thermodynamics as pointed out by Gor'kov and Eliashberg¹⁰ who were the first to introduce the $P_{n-1}^{(n)}$ distributions into the small-particle problem.

III. CANONICAL PARTITION FUNCTION AND EQUAL-LEVEL PROBLEM

For arbitrary spacing between the energy levels in a small particle the canonical partition function cannot be expressed in a closed form. Of course at temperatures such that only the lowest excitations are important, it is convenient to write out the partition function term by term, and at higher temperatures it can be calculated by the saddle-point method.² But before making any approximations, it is worthwhile to consider the case with equal level spacings where one can calculate the canonical partition function exactly.¹ Since the perturbations on the surface of a small particle are expected to break apart degenerate energy levels and produce an average level spacing δ , this problem with equal level spacing δ forms an initial approximation to the actual case. The resulting specific heat and susceptibility will be seen to differ from the grand canonical expressions. In Sec. IV this equal level solution will then be used in an approximation scheme to calculate the canonical partition function for a distribution of level spacings.

The canonical partition function is projected out of the grand canonical form by the Darwin-Fowler contour integration:

$$Q(N, \beta, H) = \frac{1}{2\pi i} \oint \frac{dz}{z^{N+1}} Q(z, \beta, H), \quad (6)$$

where

$$Q(z, \beta, H) = \prod_{\substack{i=1 \\ s=\pm 1}}^{\infty} (1 + z e^{s\hbar} e^{-\beta\eta_i}), \quad \hbar = \frac{1}{2} \beta g \mu_B H.$$

The energy levels η_i are ordered with $\eta_1 \leq \eta_2 \leq \eta_3 \dots$. It is convenient to factor out the ground state which then allows Q to be expressed in terms of particle-hole excitations. With a change of variables to measure energies from the topmost occupied level η_p at $T=0$, one obtains a form originally discussed by Kubo²:

$$Q(N, \beta, H) = e^{-\beta E_0(N)} Z(H), \quad (7)$$

with

$$Z(H) = \frac{1}{2\pi i} \oint \frac{dz}{z} z^r \prod_{\substack{i=0 \\ s=\pm 1}}^{p-1} [1 + (1/z) e^{s\hbar} e^{-\beta\epsilon'_i}] \\ \times \prod_{\substack{k=1 \\ s=\pm 1}}^{\infty} (1 + z e^{s\hbar} e^{-\beta\epsilon_k}),$$

where

$$E_0(N) = 2 \sum_{i=1}^p \eta_i - r\eta_p;$$

$$r = \begin{cases} 0 & \text{even number of electrons} \\ 1 & \text{odd number of electrons;} \end{cases}$$

$$\epsilon'_i = \eta_p - \eta_{p-i} \geq 0;$$

$$\epsilon_k = \eta_{p+k} - \eta_p \geq 0.$$

In these formulas $E_0(N)$ is the ground-state energy of $N = 2p - r$ electrons in zero magnetic field, and so $Z(H)$ still contains the H -dependent ground-state contribution. The above expression for $Z(H)$ is valid at all temperatures, but one usually calculates the integral by a steepest-descent integration; this is justified when $\beta\delta \ll 1$, where δ is the average level spacing at the Fermi surface.

However, it is also possible to perform the contour integration for all temperatures in the case of equal level spacing. For this case one has $\epsilon_k = \delta k$. Because of thermal degeneracy $p\delta\beta \gg 1$, one can extend the limits in the first group of products to infinity. After changing variables to $z' = z e^{-\hbar}$ and integrating around the unit circle, one obtains

$$Z = (4/\pi) e^{(r-1)\hbar} \int_0^\pi d\varphi e^{-2i\varphi(r-1)} \cos(\varphi - i\hbar) \cos\varphi \\ \times \prod_{k=1}^{\infty} [1 + 2 \cos 2(\varphi - i\hbar) e^{-\beta\delta k} + e^{-2\beta\delta k}] \\ \times \prod_{i=1}^{\infty} (1 + 2 \cos 2\varphi e^{-\beta\delta i} + e^{-2\beta\delta i}). \quad (8)$$

Appearing in the integrand is the product of two θ functions, $\theta_2(\varphi - i\hbar, q)$ and $\theta_2(\varphi, q)$ in their product representations, so the partition function can

be written in the form

$$Z = (q^{-1/2}/\pi G^2) \int_0^\pi d\varphi \theta_2(\varphi - i\hbar, q) \theta_2(\varphi, q) \\ \times e^{2i\varphi(r-1)} e^{(r-1)\hbar}, \quad (9)$$

with

$$q = e^{-\beta\delta/2},$$

$$G = \prod_{n=1}^{\infty} (1 - q^{2n}).$$

The θ functions satisfy the important relationship¹¹

$$\theta_2(z, q) = 2Gq^{1/4} \cos z \prod_{n=1}^{\infty} (1 + 2q^{2n} \cos 2z + q^{4n}) \\ = 2 \sum_{n=0}^{\infty} q^{(n+1/2)^2} \cos(2n+1)z. \quad (10)$$

Substituting the series expansion of θ_2 into Eq. (9) facilitates the integration over φ , and the result is

$$Z_{\text{even}}^0 = \left(1 + 2 \sum_{n=0}^{\infty} e^{-\beta\delta(n+1)^2} \cosh 2(n+1)\hbar \right) Z_B^2, \\ Z_{\text{odd}}^0 = \left(2 \sum_{n=0}^{\infty} e^{-\beta\delta n(n+1)} \cosh(2n+1)\hbar \right) Z_B^2, \quad (11)$$

with

$$Z_B = \prod_{n=1}^{\infty} (1 - e^{-\beta\delta n})^{-1}. \quad (12)$$

Here Z_B is the canonical partition function for spinless fermions, which one calculates similarly.

The form for the partition function implies that the excitations which contribute to the canonical partition function are bosonlike. In the standard grand canonical case, the excitations consist of linearly independent particle and hole excitations which, of course, lead to the usual Fermi functions. However, the restriction of electron number conservation implies that for each particle excitation there must be a corresponding hole. That within the equal-level-spacing assumption these collective particle-hole excitations lead to the boselike partition functions is in fact simply shown using a scheme originally introduced by Tomonaga.¹²

To begin with, consider a spinless fermion system with equal one-electron energy levels $k\delta$ with k running from 0 to m . In the ground state the levels will be filled up to some level p with $0 \ll p \ll m$. Then the canonically allowed excited states are generated by applying all possible particle-hole excitation operators of the form $c_k^\dagger c_{k'}$. Here $c_{k'}$ removes a particle from the $k'\delta$ state, and c_k^\dagger creates a particle in a $k\delta$ state. According to Tomonaga, one introduces in place of the $c_k^\dagger c_{k'}$ operators the linear combinations

$$a_q^\dagger = \frac{1}{\sqrt{q}} \sum_{k=0}^{m-q} c_{k+q}^\dagger c_k \quad (13)$$

and their Hermitian conjugates. Without loss of generality one may assume $q \leq q'$, and one finds then

$$[a_q, a_{q'}^\dagger] = \frac{1}{\sqrt{qq'}} \left(\sum_{k=0}^{q-1} c_{k+q'-q}^\dagger c_k - \sum_{k=m-q'+1}^{m+q-q'} c_{k+q'-q}^\dagger c_k \right). \tag{14}$$

For a degenerate, noninteracting electron system the levels 0 to $q-1$ are occupied while the levels $m-q'+1$ to $m+q-q'$ are empty for the physically significant q, q' states. Therefore, the right-hand side of Eq. (14) vanishes unless q equals q' in which case it reduces to unity, so the $a_{q'}^\dagger$ and a_q operators obey Bose commutation relations. While the degeneracy condition is usually well satisfied, the effect of the Coulomb interactions between the electrons lead to modifications of the occupation numbers which break down this simple Bose picture. However, for the present degenerate noninteracting canonical problem, Eq. (14) provides an accurate representation.

The Hamiltonian for the equal-level-spacing case is

$$H = \sum_{k=0}^m k \delta c_k^\dagger c_k. \tag{15}$$

The equal spacing of the levels leads to the commutation relation

$$[H, a_q^\dagger] = k \delta a_q^\dagger. \tag{16}$$

Therefore, the particle-hole excitations allowed in a canonical description are Bose-like with a spectrum $k\delta$. The resulting canonical partition function for this spinless fermion case is just Z_B given in Eq. (12).

In order to treat the spin case, it is useful to classify the states by their total z component of spin angular momentum S_z . For each S_z manifold, there is a state of lowest energy $E(S_z)$, and the excited states in the manifold are generated by the Tomonaga Bose operators a_{qs}^\dagger suitably generalized to the spin case

$$a_{qs}^\dagger = \frac{1}{\sqrt{q}} \sum_{k=0}^{m-q} c_{k+qs}^\dagger c_{ks}. \tag{17}$$

The contribution of this manifold to the canonical sum over states is therefore simply

$$e^{-\beta E(S_z)} Z_B^2, \tag{18}$$

where the Z_B^2 reflects the two spin degrees of freedom of the a_{qs}^\dagger excitations.

For the even-spin case the lowest energy $S_z = 0$, $S_z = 1$, and $S_z = 2$ states are illustrated in Fig. 1(a). Measured relative to the $S_z = 0$ state, the $S_z = 1$ and $S_z = 2$ states have energies $\delta + g\mu_B H$ and $4\delta + 2g\mu_B H$, respectively. In general, the lowest energy state in a given S_z manifold, measured relative to the lowest $S_z = 0$ state has an energy

$$E_{\text{even}}(S_z) = S_z^2 \delta + g\mu_B H S_z. \tag{19}$$

In a similar manner, Fig. 1(b) illustrates the lowest energy $S_z = \frac{1}{2}$, $S_z = \frac{3}{2}$, and $\frac{5}{2}$ states for an odd-electron system. The general form for the odd number of electrons is

$$E_{\text{odd}}(S_z) = \delta(S_z^2 - \frac{1}{4}) + g\mu_B H S_z. \tag{20}$$

Using Eqs. (19) and (20) in Eq. (18) and summing over $\pm S_z$ values, the canonical partition functions, Eq. (11), for the even and odd case, respectively, are obtained.

We discuss now the canonical specific heat and susceptibility, which are calculated from the partition function in Eq. (11). The results over the entire temperature range must be obtained numerically. However, one can see the qualitative features by considering the low- and high-temperature limits. At low temperatures, where one has $\beta\delta \gg 1$, only a few low-lying levels are important. The exact counting of the possible states then leads to a clear distinction between the even and odd cases. The lowest terms in the partition function are

$$Z_{\text{even}}^0 = (1 + 2e^{-\beta\delta} \cosh 2h) \times (1 + 2e^{-\beta\delta} + 5e^{-2\beta\delta} + 10e^{-3\beta\delta}) + O(e^{-4\beta\delta}), \tag{21}$$

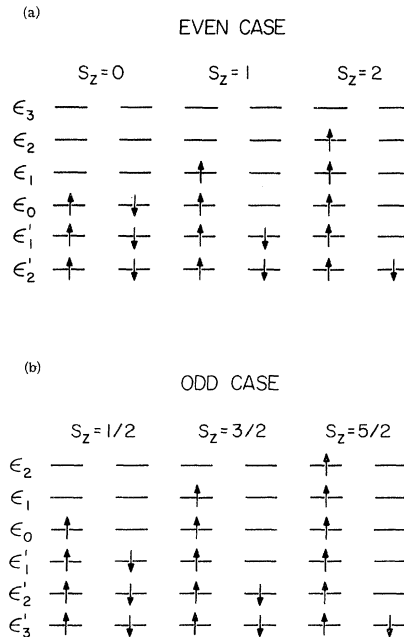


FIG. 1. (a) Lowest energy configurations for the $S_z = 0, 1$, and 2 manifolds for an even number of electrons. (b) Lowest energy configurations for the $S_z = \frac{1}{2}, \frac{3}{2}$, and $\frac{5}{2}$ manifolds appropriate to an odd number of electrons.

$$Z_{\text{odd}}^0 = 2(\cosh h + e^{-2\beta\delta} \cosh 3h) \\ \times (1 + 2e^{-\beta\delta} + 5e^{-2\beta\delta} + 10e^{-3\beta\delta}) + O(e^{-4\beta\delta}).$$

The specific heat calculated from the above is exponentially attenuated as $T \rightarrow 0$. The susceptibility will exhibit the Curie-law behavior for the odd case while the susceptibility in the even case is exponentially attenuated.

In the high-temperature limit, one has $\beta\delta \ll 1$, and there are many excited states. The exact counting of all states according to the canonical scheme then becomes less important, and the even-odd distinction washes out. With $\beta\delta \ll 1$ the logarithm of the partition function can be converted into an integral form, where the lower limit in the spinless partition function Z_B must be treated carefully. One obtains

$$\ln Z_{\text{even}}^0 = \frac{\beta(g\mu_B H)^2}{4\delta} + \frac{1}{2} \ln \frac{\pi}{\beta\delta} - 2 \int_{1/2}^{\infty} dx \ln(1 - e^{-\beta\delta x}) \\ = \ln Z_{\text{odd}}^0. \quad (22)$$

The heat capacity and susceptibility are then calculated from

$$C = k\beta^2 \frac{\partial^2 \ln Z}{\partial \beta^2} \quad \text{and} \quad \chi = \frac{1}{\beta} \frac{\partial^2 \ln Z}{\partial H^2}. \quad (23)$$

The results for both the even and odd cases are the same in this limit:

$$\frac{C}{k} = \frac{1}{2} + \frac{2}{\beta\delta} \int_{\beta\delta/2}^{\infty} dx \frac{x^2 e^x}{(e^x - 1)^2} = \frac{2\pi^2}{3} \frac{kT}{\delta} - \frac{1}{2}, \\ \chi = 2\left(\frac{1}{2}g\mu_B\right)^2 / \delta. \quad (24)$$

This is just the usual Pauli spin susceptibility, but the linear law in the specific heat is corrected by the term $-k/2$. This added term in the specific heat can also be calculated as the first higher-order term in a steepest-descent integration of the partition function given in Eq. (7); however, since the correction is of order $1/N$ (where N = electron number) compared to the linear term in the specific heat, it is usually neglected. Nevertheless, for the canonical ensemble these corrections of order one are important at low temperatures $kT \lesssim \delta$, since the specific heat per metal particle is only of this order. Of course, experimentally one deals with samples containing 10^{14} or more particles.

The heat capacities computed numerically from Eq. (11) for $H = 0$ are shown in Fig. 2(a) together with the grand canonical results which essentially have been obtained by Fröhlich in 1937.¹³ The canonical and grand canonical susceptibilities also differ; these are shown in Fig. 2(b). Notice the odd case leads to a Curie-law behavior at sufficiently low values of kT/δ due to the unpaired spin, while the susceptibility in the even case is exponentially at-

tenuated. At higher values of kT/δ both even and odd cases approach the Pauli susceptibility.

It is evident that the grand canonical ensemble gives rise to a larger heat capacity at all temperatures; this follows since there are more excitations allowed when the electron number is not conserved. In the case of even electron number, the chemical potential is between the topmost occupied level and the next empty level (at $T = 0$). Therefore the smallest grand canonical excitations have an energy $\frac{1}{2}\delta$, and the heat capacity is attenuated like $e^{-\beta\delta/2}$ instead of $e^{-\beta\delta}$ as seen in Fig. 2(a). In contrast, for odd electron number the chemical potential occurs at the topmost occupied level which in turn explains a low-temperature behavior $\sim e^{-\beta\delta}$ similar to the canonical heat capacities.

The difference between the canonical and grand canonical ensembles becomes quite obvious by comparing the mean occupation numbers. In order to obtain the Fermi function from the canonical partition function of Eq. (7), one must assume the usual thermodynamic limit $\beta\delta = \delta/kT \ll 1$. This allows one to make an asymptotic evaluation; in so

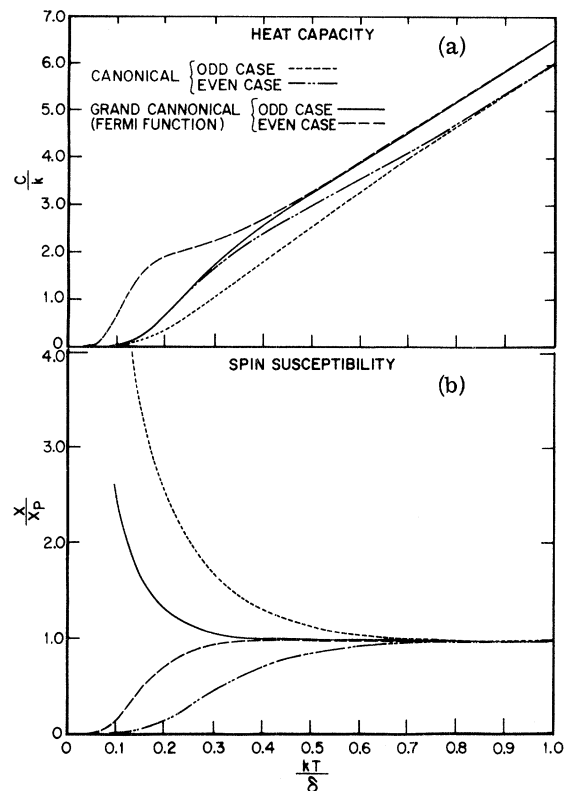


FIG. 2. (a) Comparison of the specific heat calculated for the equal level model using the canonical ensemble with that calculated using the grand canonical ensemble. (b) Comparison of the canonical and grand canonical spin susceptibility, with the results normalized to the Pauli spin susceptibility.

doing corrections of order $1/N$ are neglected. Therefore, one might expect the Fermi function to adequately describe the canonical occupation number only as $\beta\delta$ becomes small, the condition which is assumed in its derivation. To see this quantitatively we calculate the canonical occupation number for arbitrary values of the parameter $\alpha = \beta\delta$. For the sake of simplicity, we confine our attention here to the case of spinless fermions. Their canonical partition function is

$$Z_B = \frac{1}{2\pi i} \oint \frac{dz}{z} \prod_{k=1}^{\infty} (1 + ze^{-\beta\epsilon_k}) \prod_{i=0}^{N-1} \left(1 + \frac{1}{z} e^{-\beta\epsilon_i'}\right), \quad (25)$$

from which the canonical mean occupation numbers follow:

$$\begin{aligned} \langle n_k \rangle &= -\frac{\partial}{\partial(\beta\epsilon_k)} \ln Z_B, \\ \langle n_i' \rangle &= -\frac{\partial}{\partial(\beta\epsilon_i')} \ln Z_B. \end{aligned} \quad (26)$$

By performing the differentiations and using the θ function given in Eq. (10) for the equal level system, we obtain for the canonical particle-hole distribution function

$$\begin{aligned} n(|x|) &= \frac{1}{\pi} e^{\alpha/8} \int_0^{\pi} d\varphi \theta_2(\varphi, e^{-\alpha/2}) \frac{e^{-i\varphi}}{e^{i\pi|\alpha/2 - 2i\varphi} + 1} \\ &= \sum_{p=0}^{\infty} (-1)^p \exp\left[-\frac{1}{2}\alpha(p+1)^2 - (p+1)|x|\right], \end{aligned} \quad (27)$$

where

$$\alpha = \beta\delta, \quad x = x_m = \alpha(m - \frac{1}{2}),$$

$$m = \begin{cases} 1, 2, 3, \dots, & \text{particles} \\ 0, -1, -2, \dots, & \text{holes.} \end{cases}$$

The series expansion is a further consequence of Eq. (10).

On the other hand, the Fermi function for a spinless equal level system is $f(x_m) = (e^{x_m} + 1)^{-1}$, where at $T=0$ levels with $m \leq 0$ are filled and levels with $m \geq 1$ are empty. With $m \leq 0$ the probability of finding a hole is $1 - f(x_m)$. Therefore, in terms of particle-hole excitations the grand canonical occupation numbers are

$$f(|x_m|) = 1/(e^{|x_m|} + 1), \quad (28)$$

where $m \leq 0$ corresponds to holes and $m \geq 1$ corresponds to particles. Comparing the geometrical series for $f(|x|)$ with the series expansion of $n(|x|)$, we immediately recognize that the canonical particle-hole distribution $n(|x|)$ approaches the grand canonical Fermi function as $\alpha = \delta/kT$ tends to zero.

An interesting formal relationship between the canonical and grand canonical occupation functions can be obtained by observing that $n(x, \alpha)$, defined

by Eq. (27) with $|x|$ replaced by x satisfies the diffusion equation

$$\frac{1}{2} \frac{\partial^2 n}{\partial x^2} - \frac{\partial n}{\partial(-\alpha)} = 0, \quad (29)$$

where we assume that x and α are treated as independent continuous variables. Then since $n(|x|, 0) = f(|x|)$, it follows that

$$f(|x|) = \int_{-\infty}^{\infty} \frac{\exp[-(x' - |x|)^2/2\alpha]}{(2\pi\alpha)^{1/2}} n(x', \alpha) dx'. \quad (30)$$

This implies that in passing from the canonical to the grand canonical ensemble by removing the constraint of number conservation, one arrives at the familiar Fermi function by a "diffusive" process. Mathematically, this observation is easily understood since the θ function (which, as we have seen, is intimately connected with the canonical statistics of the equal level system) itself obeys the diffusion equation.¹¹ The "physical" values for x in $f(|x|)$ are still $x = x_m$ from Eq. (27).

The canonical occupation number $n(x)$ has been calculated directly by using the series expansion of Eq. (27), and the results are compared to the Fermi function in Fig. 3. It is seen that $f(x)$ always lies above $n(x)$ for $x > 0$, corresponding to the larger number of particle excitations in the grand canonical ensemble. For $x < 0$, corresponding to hole excitations, the results have been

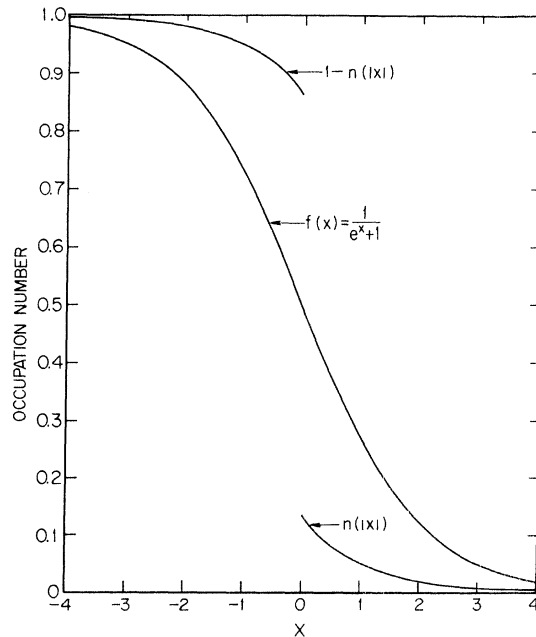


FIG. 3. Comparison of the grand canonical Fermi function $f(x)$ with the canonical mean occupation number $n(x)$, for $\delta/kT=4$. The curve has meaning only at the positions of the equally spaced energy levels which are given by $\epsilon_m/kT = x_m = \delta(m - \frac{1}{2})/kT$, with $m = 0, \pm 1, \pm 2, \dots$

plotted as $f(x) = 1 - f(|x|)$ and $1 - n(|x|)$; this allows a more direct comparison of the canonical occupation and the Fermi function $f(x)$. In this case the greater probability for hole excitations in the grand canonical ensemble results in its occupation number being smaller than that of the canonical ensemble. Analogous results also hold for the system with spin, but this simple case is sufficient to illustrate the importance of carefully treating the canonical occupation numbers or the actual number of excitations at sufficiently low temperatures.

The solution to the equal level problem also displays an interesting periodicity. As the magnetic field is increased from zero, the energy levels with spins aligned parallel to the field direction will be raised compared to the levels with spins antiparallel. Increasing H thus alters the contributions of the various total spin manifolds to $Z(H)$, and both the specific heat and susceptibility are changed. When H is increased to the point that $\frac{1}{2}g\mu_B H = \delta$, the levels are brought into coincidence again, and the specific heat and susceptibility become the same as for $H=0$. This process repeats itself as one continues to increase H . Furthermore, the even and odd cases are "converted" into one another as $\frac{1}{2}g\mu_B H$ is increased from 0 to $\frac{1}{2}\delta$, without changing the number of electrons! Mathematically, this follows from the expression for $Z(H)$ in terms of θ functions given in Eq. (10). The θ function is "quasidoubly periodic":

$$\begin{aligned} \theta_2(z + \pi, q) &= -\theta_2(z, q), \\ \theta_2(z \pm \frac{1}{2}i\alpha, q) &= (1/q) e^{\mp 2i z} \theta_2(z, q) \text{ for } q = e^{-\alpha/2}. \end{aligned} \quad (31)$$

Although the periodicity of the first expression is exhausted in the integration over the φ variables in Eq. (9), the second periodicity leads to the following relation between the even and odd cases in a magnetic field:

$$\begin{aligned} Z_{\text{even}}^0(\alpha, h + \frac{1}{2}\alpha) &= e^h Z_{\text{odd}}^0(\alpha, h), \\ Z_{\text{odd}}^0(\alpha, h + \frac{1}{2}\alpha) &= e^{h+\alpha/2} Z_{\text{even}}^0(\alpha, h), \end{aligned} \quad (32)$$

$$\alpha = \beta\delta, \quad h = \frac{1}{2}\beta g\mu_B H.$$

The exponential factors can be neglected, at least in calculating the specific heat and spin susceptibility, since these involve second derivatives of $\ln Z$. Therefore, for the two cases Z_{even}^0 and Z_{odd}^0 one only needs to calculate the specific heat and susceptibility over the range $0 \leq \frac{1}{2}g\mu_B H \leq \frac{1}{2}\delta$, and the results can then be periodically extended to all values of H .

The magnetization has been calculated first, using the partition function of Eq. (11). The results for two values of temperature are shown in Fig. 4, where it is seen that the curves smooth out rapidly as the parameter kT/δ increases. The first transitions, corresponding to increases in the magnetization as $\frac{1}{2}g\mu_B H/\delta$ increases, are indicated in the inset. The specific heat and spin susceptibility have also been calculated as a function of H for fixed values of kT/δ , using the partition function of Eq. (11). The resulting periodicity for this equal level system is displayed in Figs. 5(a) and 5(b) where the magnetic field H is measured in units of $\frac{1}{2}g\mu_B H/\delta$. In agreement with Eqs. (32), it is seen that the behavior is periodic in H with period $2\delta/g\mu_B$. A small value for kT/δ has been chosen

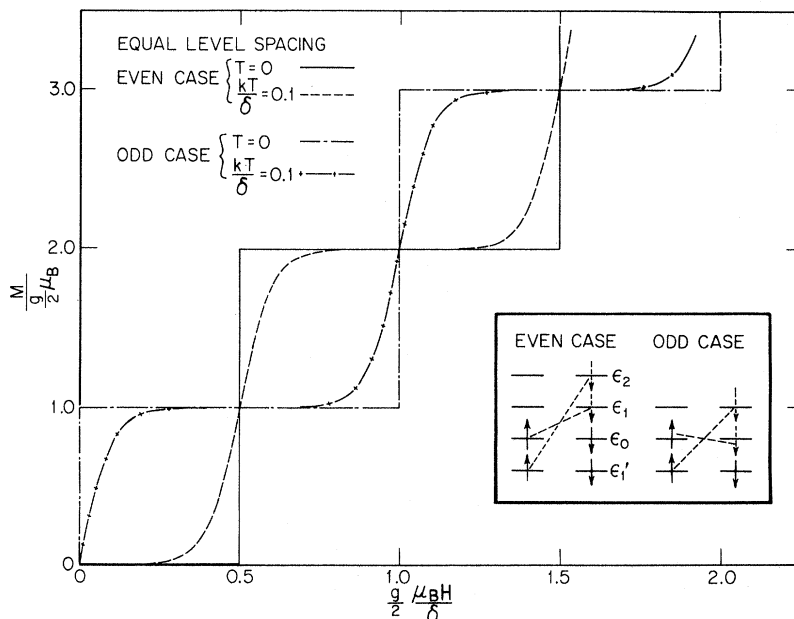


FIG. 4. Magnetization calculated from the canonical partition function as a function of $g\mu_B H/2\delta$, for temperatures $T=0$ and $kT/\delta=0.1$. The inset shows the first spin-flip transitions.

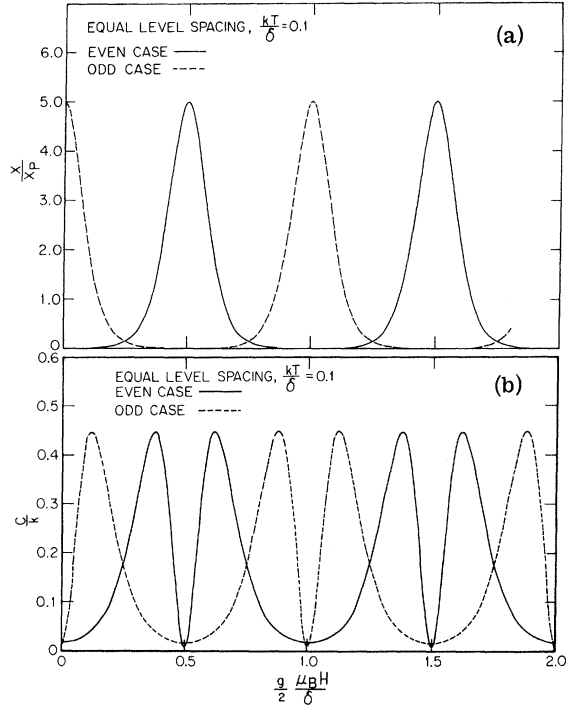


FIG. 5. (a) Periodicity in the spin susceptibility as a function of $g\mu_B H/2\delta$, for the value $kT/\delta = 0.1$. The susceptibility is normalized to the Pauli value. (b) Periodicity in the specific heat as a function of $g\mu_B H/2\delta$, again for the value $kT/\delta = 0.1$.

in order to emphasize the periodicity. As kT/δ is increased the contribution of the spin-flip terms to the specific heat, which leads to the periodicity, remains small and becomes negligible compared to the non-spin-flip contribution calculated from Z_B^2 . Also in the case of the spin susceptibility the "sharp" periodic behavior is most evident when kT/δ is small. As kT/δ becomes large the average of the odd and even cases approaches the Pauli susceptibility as a limit.

Concluding this section, we want to study a simple example of an interaction. Here we add a short-ranged-model Coulomb energy

$$H_{\text{int}} = U \sum_{kk'} n_{k\uparrow} n_{k'\uparrow} = UN_1 N_1 = U(\frac{1}{4}N^2 - S_z^2) \quad (33)$$

to the free system of N electrons in order to study the effect of exchange correlations within the framework of the canonical ensemble. The additional energy can be included in the expression for $E(S_z)$ used previously, Eq. (18), to calculate the canonical partition function, and we find

$$Z_{\text{even}}^0 = e^{-\beta U N^2/4} \times \sum_{S_z=0, \pm 1, \pm 2, \dots} \exp[-\beta \delta (1 - U/\delta) S_z^2 - 2S_z h] Z_B^2, \quad (34)$$

$$Z_{\text{odd}}^0 = e^{-\beta U (N^2-1)/4} \times \sum_{S_z=\pm 1/2, \pm 3/2, \pm 5/2, \dots} \exp[-\beta \delta (1 - U/\delta) (S_z^2 - \frac{1}{4}) - 2S_z h] Z_B^2.$$

Incorporating the S_z -independent factors outside the summation into the ground-state energy, the partition functions reduce to expressions similar in form to the noninteracting case:

$$Z_{\text{even}}^0 = \left(1 + 2 \sum_{n=0}^{\infty} e^{-\beta \bar{\delta} (n+1)^2} \cosh 2(n+1)h \right) Z_B^2(\bar{\delta}),$$

$$Z_{\text{odd}}^0 = \left(2 \sum_{n=0}^{\infty} e^{-\beta \bar{\delta} n(n+1)} \cosh(2n+1)h \right) Z_B^2(\bar{\delta}), \quad (35)$$

$$Z_B(\bar{\delta}) = \prod_{n=1}^{\infty} (1 - e^{-\beta \bar{\delta} n})^{-1},$$

where

$$\bar{\delta} = \delta(1 - U/\delta).$$

This result is interesting in that it corresponds to the susceptibility being renormalized by the familiar Stoner factor $(1 - U/\delta)^{-1}$ which enhances the bare density of states δ^{-1} to $\bar{\delta}^{-1}$, whereas the specific heat still has a dependence on both δ and $\bar{\delta}$. Limiting forms for the specific heat and susceptibility can be calculated when either $\beta\bar{\delta} \ll 1$ or $\beta\delta \ll 1$, just as in the noninteracting case already treated. Since $\bar{\delta} < \delta$, consider first a temperature such that $\beta\bar{\delta} \ll 1$. The partition functions for the even and odd cases become equal and are

$$\ln Z^0 = 2 \ln Z_B(\beta\bar{\delta}) - \frac{1}{2} \ln \beta\bar{\delta} + h^2/\beta\bar{\delta} + \text{const.} \quad (36)$$

At a somewhat higher temperature such that $\beta\delta \ll 1$, one can also convert the spinless partition function Z_B to integral form, and the partition function becomes

$$\ln Z^0 = \ln \beta\delta + \pi^2/3\beta\delta - \frac{1}{2} \ln \beta\bar{\delta} + h^2/\beta\bar{\delta} + \text{const.} \quad (37)$$

In the limit $H=0$, Eqs. (35) for Z correspond to specific heats and susceptibilities given by

$$C/k_B = \frac{1}{2} + 2 \sum_{p=1}^{\infty} \frac{(\beta\delta p)^2 e^{-\beta\delta p}}{(1 - e^{-\beta\delta p})^2}, \quad \beta\bar{\delta} \ll 1$$

$$= \frac{2\pi^2}{3} \frac{kT}{\delta} - \frac{1}{2}, \quad \beta\bar{\delta} \ll 1, \quad \beta\delta \ll 1; \quad (38)$$

$$\chi = \frac{2(g\mu_B/2)^2}{\delta(1 - U/\delta)}, \quad \beta\bar{\delta} \ll 1.$$

The susceptibility exhibits the Stoner factor, but note also when $\beta\bar{\delta} \ll 1$ but $\beta\delta \gg 1$, the specific heat approaches the value $\frac{1}{2}$ for this strongly exchange-enhanced case, since it costs less and less energy for the spins to flip and give higher values of S_z . This behavior for the specific heat can be seen in Fig. 6, where A is defined as $A = \bar{\delta}/\delta = 1 - U/\delta$, with A going to zero as the exchange interaction increases. The effect of the interaction is to decouple the spin-flip and non-spin-flip contributions;

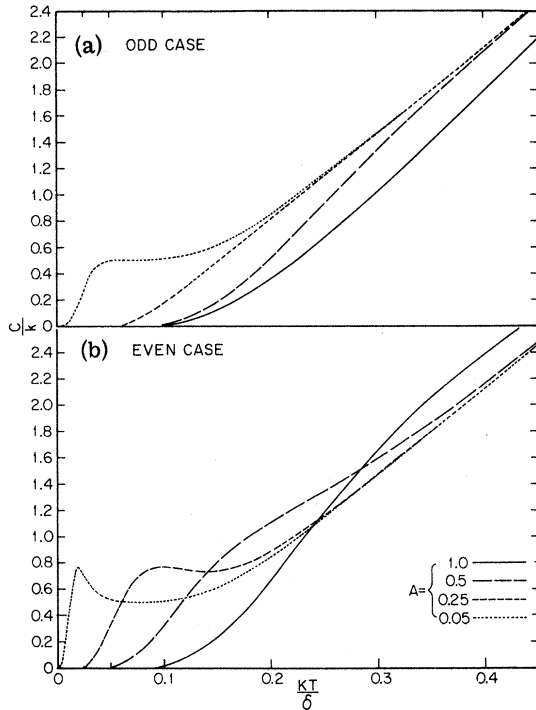


FIG. 6. (a) Specific heat for the case with an odd number of conduction electrons, for several values of the parameter A . The value of δ is given by $\delta = A\delta$; hence, a decrease in the value of A from unity corresponds to turning on the short-ranged interaction. (b) Specific heat in the even case, for the same values of A as in Fig. 6(a).

for increasing exchange coupling these spin-flip terms are scaled to contribute closer to $T=0$. As can be seen, the spin-flip terms in the odd case monotonically reach a contribution of $\frac{1}{2}$, while these terms in the even case give an anomalous contribution before approaching the limiting value $\frac{1}{2}$. As A increases to 1, the scale is such that the anomalous contribution is very broad, so that it is barely noticeable.

IV. LEVEL DISTRIBUTION AVERAGE

We now turn to the general problem of calculating the specific heat and susceptibility where equal level spacing no longer applies. The formal solution requires an average of the energy levels over the probable distribution of levels for the small particles, so the statistical distributions discussed in Sec. II will be applied in this section. For very low temperatures, when only one or two levels are involved, the results can be obtained analytically.^{2,10} However, one desires a means of calculating the specific heat and susceptibility for all temperatures, and this will require a numerical solution. The solution will be compared with the analytic results for low temperature, which allows a determination of the temperature range over which

the low-temperature results remain valid. The approximation method developed for calculating this solution will utilize the equal level solution of Sec. III, and will involve an average over just a few levels close to the Fermi level.

But before considering any approximations, it is interesting to note that one can avoid numerical methods in showing how the periodicity of the susceptibility discussed in Sec. III is smeared out when the levels are "randomized." For this purpose the low-temperature susceptibility for the case of negligible spin-orbit coupling will be considered. Here the orthogonal ensemble is appropriate, and it is convenient to introduce the probability functions $p_n(x)$, where $p_n(x)$ is defined as the probability that two energy levels are a spacing x apart with n levels in between them (x is normalized to the average spacing between two adjacent levels: $x = \epsilon/\delta$). In terms of the p_n functions,¹⁴ the probability $R(x)$ of finding two levels a spacing x apart regardless of the position of the other levels is

$$R(x) = \sum_{n=0}^{\infty} p_n(x).$$

At small x , $R(x)$ varies as $P_0(x)$ and for $x > 1$, $R(x)$ approaches unity. A general expression for $R(x)$ has been obtained by Dyson.⁶

At very low temperatures as H increases, there will be abrupt changes in the spin magnetism and thus large values for the susceptibility at the points when it is energetically favorable for a spin to flip; representative energy levels are sketched in Fig. 7. One can show in applying the canonical partition function at these low temperatures that the susceptibility reduces to pairwise contributions corresponding to the possible "transitions" in the figure, with each contribution behaving like the derivative of a Fermi function. These pairs of levels are averaged over the appropriate distribution p_n describing the probable spacing between them. For example, in the odd case levels 1 and 1' are averaged over p_1 , levels 2 and 2' are averaged over p_3 , etc. Similarly in the even case one uses p_0, p_2, p_4 , etc. Finally, if a simple average (appropriate for a collection of small particles) of the even and odd cases is taken, one obtains:

$$\chi_{ave} = \frac{(\frac{1}{2}g\mu_B)^2}{2kT} \operatorname{sech}^2(\frac{1}{2}\beta g\mu_B H) + \frac{2(\frac{1}{2}g\mu_B)^2}{\delta}$$

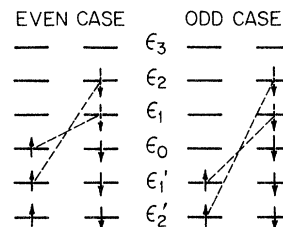


FIG. 7. First spin-flip transitions, for an even and odd number of conduction electrons.

$$\times \left\{ R \left(\frac{g\mu_B H}{\delta} \right) + \frac{\pi^2}{6} \left[\frac{d^2 R(\epsilon/\delta)}{d\epsilon^2} \right]_{\epsilon=g\mu_B H} (kT)^2 + \dots \right\}. \quad (39)$$

The first term, apart from the 2 which arises from averaging the even and odd cases, comes from the unpaired spin in the odd case. As $g\mu_B H$ increases past δ , R goes to 1 and its second derivative goes to zero, so one just has the Pauli paramagnetism with no periodic effects. The behavior of the susceptibility has also been described by Gor'kov and Eliashberg, who calculated just the second term in the equation above.

To calculate the specific heat and susceptibility for a collection of small particles, one must start with the appropriate partition function. For $H=0$ the statistical distribution of levels is described by the orthogonal ensemble for weak spin-orbit coupling, and the symplectic ensemble describes the level distribution as this coupling is increased. Both of these ensembles have levels which are twofold degenerate; for the orthogonal ensemble there are two spin directions, and in the symplectic case there is the twofold Kramers degeneracy. Therefore, in these cases the canonical partition function of Eq. (7) is appropriate, where the magnetic field H is set equal to zero. On the other hand, with both a sufficiently large magnetic field present and spin-orbit coupling, the unitary ensemble describes the energy-level distribution. In this case there is no longer any energy-level degeneracy since the previously twofold degenerate levels with average level spacing δ are split apart, which produces a system with average level spacing $\frac{1}{2}\delta$. In this case the partition function would be that appropriate to a spinless system, and there would no longer be any even-odd distinction. Finally, for comparison with the orthogonal and symplectic results, we will also consider the random distribution of energy levels (Poisson distribution) which was first used by Kubo.² For this case the levels are taken to be twofold degenerate for $H=0$, so the partition function in Eq. (7) will be used again.

Once the partition function Z is specified, its logarithm must be averaged over the statistical distribution describing the levels in the collection of particles. The statistical average of $\ln Z$ is denoted as $\langle \ln Z \rangle$. In the partition function the energy levels ϵ_i and ϵ'_i are ordered with respect to the Fermi level ϵ_0 , where the ϵ_i referred to particles above ϵ_0 and ϵ'_i referred to holes. The ground-state energy is chosen to give $\epsilon_0=0$. In carrying out the numerical calculation, it is convenient to use as variables the energy-level spacings Δ_i defined as

$$\begin{aligned} \Delta_i &= \epsilon_i - \epsilon_{i-1} \geq 0, \\ \Delta'_i &= \epsilon'_i - \epsilon'_{i-1} \geq 0. \end{aligned} \quad (40)$$

Since the average level spacing at the Fermi surface is δ , the Δ_i will appear in the dimensionless form $x_i = \Delta_i/\delta$. The zero-field partition function $Z(\dots, \beta\epsilon'_1, \beta\epsilon_1, \dots)$ can be written in terms of the x_i as $Z(\dots, x'_1, x_1, \dots; \beta\delta)$. Setting all the x_i equal to one would then correspond to the equal level case treated in Sec. III.

The calculation of the specific heat for the collection of small particles will be considered in detail, and the susceptibility calculation is similar. Since the statistical averaging is done numerically, instead of calculating from $\langle \ln Z \rangle$, it is more convenient to average the thermodynamic quantities directly. Denoting the statistical average over the specific heat as $\langle C \rangle$, one has

$$\begin{aligned} \frac{\langle C \rangle}{k} &= \beta^2 \int_0^\infty \dots \int_0^\infty \left(\frac{\partial^2}{\partial \beta^2} \ln Z(\dots, x'_1, x_1, \dots; \beta\delta) \right) \\ &\quad \times W^{(\eta)}(\dots, x'_1, x_1, \dots) \dots dx'_1 dx_1 \dots \end{aligned} \quad (41)$$

Here $W^{(\eta)}$ is the spacing distribution obtained from the eigenvalue distribution $W_N^{(\eta)}$ in Eq. (1), and we have dropped the N index since the $N \rightarrow \infty$ limit is implicit.

In order to develop a suitable approximation method for evaluating the level ensemble averages of thermodynamic quantities such as Eq. (41), we consider first the low- and high-temperature limits. In the low-temperature limit ($\beta\delta \gg 1$) the populations of only the lowest levels in the partition function are important, and the integration of $W^{(\eta)}$ over the remaining variables in Eq. (41) yields the exact distribution functions $P_n^{(\eta)}$ of these lowest level spacings. Consider as an illustration the even case at extreme low temperatures where only the level ϵ_1 is significantly populated. In this case, the integration of $W^{(\eta)}$ over all x, x' except x_1 yields the exact nearest-neighbor spacing distribution $P_0^{(\eta)}(x)$. The partition function Z for the single level ϵ_1 is given by

$$Z = 1 + 4e^{-\beta\epsilon_1} + e^{-2\beta\epsilon_1}. \quad (42)$$

Therefore Eq. (41) becomes in this limit

$$\frac{\langle C \rangle}{k} = \beta^2 \frac{\partial^2}{\partial \beta^2} \int_0^\infty dx P_0^{(\eta)}(x) \ln(1 + 4e^{-\beta\epsilon_1} + e^{-2\beta\epsilon_1}). \quad (43)$$

The averaging over possible values of x then removes the exponential decrease in C/k for $kT/\delta \ll 1$ and produces a power-law behavior in T . The lowest-order term in $kT/\delta = 1/\beta\delta$ is given by replacing $P_0^{(\eta)}(x)$ with its leading behavior, Eq. (3), for $x \ll 1$. The resulting low-temperature behavior of the specific heat and susceptibility for the different ensembles is listed in Table I. Of course, at this point it is not evident how large kT/δ can become for the leading low-temperature behavior to remain valid.

TABLE I. Leading low-temperature behavior of the electronic heat capacity and spin susceptibility for different ensembles, with even and odd electron number.

	Even	Odd
	C/k	
Poisson	$5.02kT/\delta$	$3.29kT/\delta$
Orthogonal	$3.02 \times 10^4(kT/\delta)^2$	$1.78 \times 10^4(kT/\delta)^2$
Symplectic	$3.18 \times 10^4(kT/\delta)^5$	$1.64 \times 10^4(kT/\delta)^5$
Unitary	$5.88 \times 10^2(kT/\delta)^3$	
	χ	
Poisson	$3.04(\frac{1}{2}g\mu_B)^2/\delta$	$(\frac{1}{2}g\mu_B)^2/kT$
Orthogonal	$7.63(\frac{1}{2}g\mu_B)^2kT/\delta^2$	
Symplectic	$2.02 \times 10^3(\frac{1}{2}g\mu_B)^2(kT/\delta)^4/\delta$	

In the high-temperature limit $kT > \delta$, there are many thermal excitations present. In fact, one can show for the equal level canonical system that energy levels up to $E = 25\delta$ contribute to the specific heat for $kT \sim \delta$. This is because of the large multiplicity of the higher energy levels. For example, for the equal level model, the multiplicity of states with $E = 25\delta$ is of order 10^5 . With such a large number of levels involved, the high-temperature behavior of averages such as the specific heat, Eq. (41), are insensitive to the fine details of the actual level distributions, and only the existence of an average level spacing δ is important. Therefore when $kT > \delta$, the distribution averages approach the canonical equal-level-spacing results discussed in Sec. III. This convergence to the equal level results is, in fact, quite rapid for the Dyson ensembles because of the level repulsion effects which statistically favor level spacing of δ .

Thus the high-temperature limit approaches the equal-level-spacing results and the low-temperature behavior depends only upon the low-lying states. Therefore, a useful interpolation scheme consists of removing the low-lying states and averaging their contribution over the appropriate distributions while replacing the higher-energy states with their equal level values. For this purpose, it is useful to classify a many-electron excited state of energy E by its corresponding "equal level energy" \bar{E} . \bar{E} for a state is obtained by setting each of the single-particle levels which contribute to it equal to its equal-level-spacing value. For example, if $E = \epsilon_1 + \epsilon'_1 + \epsilon_2$, then $\bar{E} = 4\delta$.

The n th-order approximation is given by taking the appropriate statistical average over the spacings appearing in all energy levels with $\bar{E} \leq n\delta$ and setting all spacings appearing in levels with $\bar{E} > n\delta$ equal to their average value δ , including those spacings Δ_i which were present and therefore averaged over in the states with $\bar{E} \leq n\delta$. Since n adjacent level spacings are involved in the n th-order approximation, only the distribution function for n spacings is required for the averaging. This makes the problem tractable because one now integrates

over a spacing distribution with only a small number of spacings, and furthermore, one is not required to keep track of a Δ_i through the many combinations in which it appears in all the various possible excited many-electron states. Within this scheme, the "zero-order" approximation is just the equal level case. The method is illustrated below for a particle with an even number of electrons.

The first-order approximation involves averaging over the nearest-neighbor state ϵ_1 of the Fermi level:

$$\left\langle \frac{C}{k} \right\rangle = \beta^2 \int_0^\infty dx_1 P_0^{(n)}(x_1) \left(\frac{\partial^2}{\partial \beta^2} \ln Z_{\text{even}}(x_1; \beta\delta) \right). \quad (44)$$

The notation $Z(x_1; \beta\delta)$ is meant to imply all Δ_j including $\Delta_1 = \epsilon_1 - \epsilon_0$ appearing in states with $\bar{E} > \delta$ are set equal to δ , which corresponds to $\epsilon_j = j\delta$ for $\epsilon_1, \epsilon_2, \dots$. Thus the averaging over Δ_1 is limited to the state with $\bar{E} = \delta$. The next order of approximation for the even-electron case takes into account states with equal level energies $\bar{E} = 3\delta$. This is third order, according to our convention, and involves the energy-level differences $\Delta_2 = \epsilon_2 - \epsilon_1$ and $\Delta'_1 = \epsilon'_1 - \epsilon_0$. Once again, replacing all excited states having $\bar{E} > 3\delta$ by their equal level values and integrating Eq. (41) over all single-particle variables except for $\Delta_2 = \epsilon_2 - \epsilon_1$, $\Delta_1 = \epsilon_1 - \epsilon_0$, and $\Delta'_1 = \epsilon'_1 - \epsilon_0$, we obtain the third-order approximation

$$\left\langle \frac{C}{k} \right\rangle = \beta^2 \int_0^\infty \int_0^\infty \int_0^\infty dx'_1 dx_1 dx_2 P_2^{(n)}(x'_1, x_1, x_2) \times \frac{\partial^2}{\partial \beta^2} \ln Z_{\text{even}}(x'_1, x_1, x_2; \beta\delta). \quad (45)$$

The odd-electron case is handled in a similar manner; however, both Δ_1 and Δ'_1 are important at low temperatures; holes and particles enter in a more symmetrical fashion than in the even case. Therefore, instead of integrating over just Δ_1 , both Δ_1 and Δ'_1 must be averaged to guarantee the correct leading low-temperature behavior. In higher order, the odd-electron case involves approximations of the fourth, sixth, ... order.

In practice, only the first several orders of approximation have been carried out. Furthermore, we have used the approximation forms for $P_{n-1}^{(n)}$ discussed in the Appendix. As discussed there, the approximate distributions are unlikely to contribute more than a few percent error, and the major error is associated with the finite- n approximation. In order to check this for the specific heat, the even case with a distribution of energy levels given by the orthogonal ensemble has been considered. The numerical integrations for the first- and third-order approximations have been carried out. Figure 8 shows the specific heat calculated in these approximations, together with the equal-level-

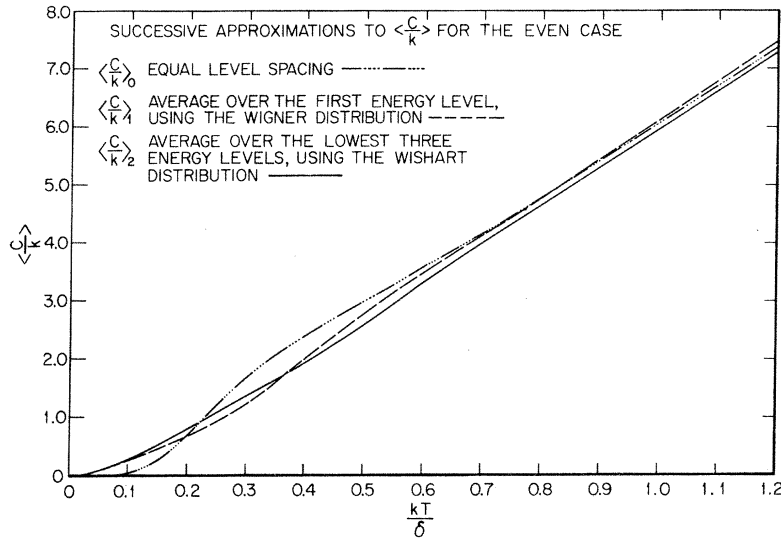


FIG. 8. Successive approximations to the specific heat in the even case, corresponding to the first-order and third-order approximations discussed in the text. The equal-level-spacing (canonical) specific heat is shown for reference.

spacing solution. As can be seen in the figure, the initial extrapolation between the low- and high-temperature behavior is reasonably smooth, and this linearity is improved as the order of the approximation increases. By the third-order approximation it is clear that nothing anomalous appears in the extrapolation between low and high temperatures. One can compare these results with the leading low-temperature behavior in Table I to estimate how large kT/δ can be for the leading low-temperature behavior to be appropriate: This turns out to be $kT/\delta \approx 0.1$. Since the leading low-temperature behavior for the other ensembles has a similar limited range of validity, experimental confirmation of the low-temperature power-law behavior of the specific heat will involve measurements in the region $kT < 0.1\delta$.

In Fig. 9 a simple average of the C_{odd} and C_{even} results is plotted for the orthogonal, symplectic, and random-energy-level distributions. The specific-heat results for the unitary level distribution are also shown on the graph. As discussed earlier in the section, one uses the partition function corresponding to spinless fermions for this ensemble. The appropriate average spacing is $\frac{1}{2}\delta$, which results from the twofold-degenerate levels in the symplectic distribution with spacing δ breaking apart as the field H is increased. Apart from the orthogonal case discussed above, only the first-order approximations were calculated for the even case, while the second-order approximations were calculated for the odd case. For temperatures larger than δ/k the heat capacities for the various distributions all converge to a linear behavior which is $\frac{1}{2}k$ lower than the familiar grand canonical result. The blowup of the low-temperature region in Fig. 9 clearly shows the difference between the

distributions. The finite probability of infinitesimal level spacings in the Poisson distribution gives rise to a low-temperature linear specific heat

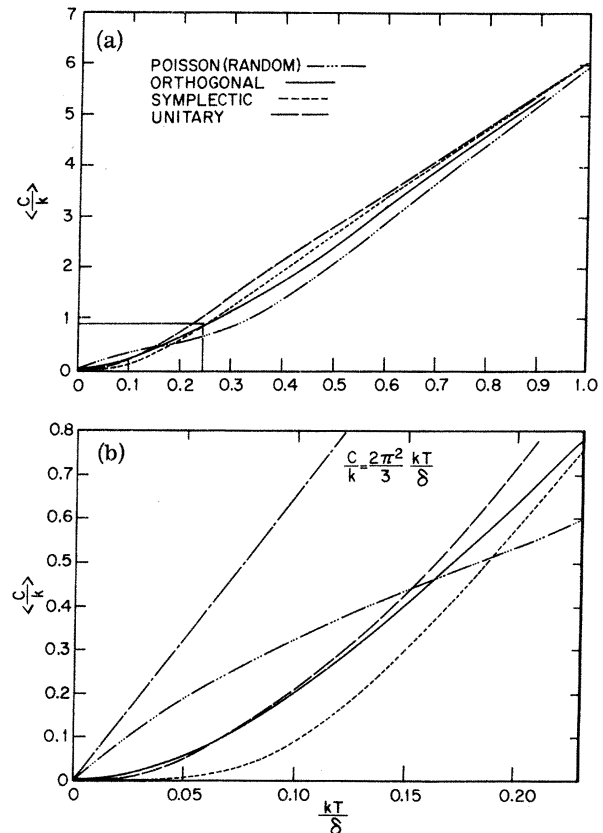


FIG. 9. (a) Resulting specific heat after averaging over the level distributions. A simple average of the results for the even and odd cases has been taken. (b) Blow-up of the specific heat for the region $0 \leq kT/\delta \leq 0.23$.

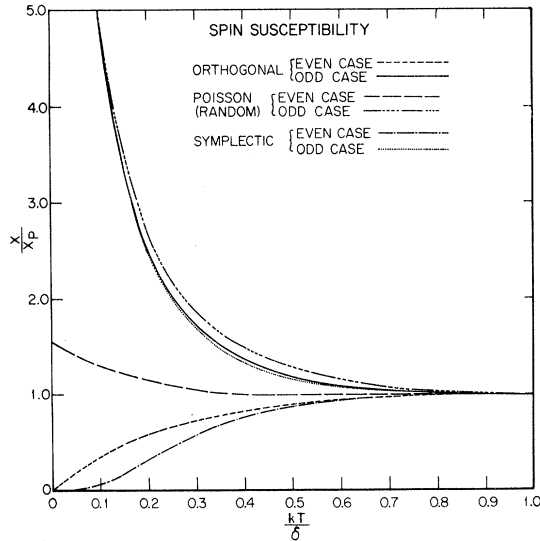


FIG. 10. Spin susceptibility resulting from an average over the level distributions, normalized to the Pauli value $\chi_p = 2(g\mu_B/2)^2/\delta$.

similar to that of the bulk metal. The energy-level correlations implicit in the other distributions are responsible for the higher-power-law behavior at low temperatures. The level repulsion effects are largest when spin angular momentum is not conserved and the Kramers degeneracy is present. This is evident in comparing the orthogonal and unitary results with those obtained from the symplectic ensemble.

The zero-field limit for the spin susceptibility has been calculated using the random, orthogonal, and symplectic level distributions. For negligible spin-orbit coupling the orthogonal ensemble is appropriate, where the g factor is 2. When the spin-orbit coupling becomes sufficiently strong, the symplectic ensemble must be used. In this case the susceptibility then depends on the effective g value of the Kramers states which are split apart by the magnetic field. The results are shown in Fig. 10, where only the lowest-order approximations were calculated. The unitary case has not been calculated since it is not appropriate for $H \approx 0$.

Just as in the equal-level-spacing case, the extra electron in the odd case gives rise to a Curie-law behavior for $kT \ll \delta$. The difference between the distributions is clearly evident in the even case. Here the finite density of states at vanishing level spacing characteristic of the random distribution gives a finite value for χ_{even} when $kT \ll \delta$. However, the level repulsion effect contained in the other distributions leads to a spin susceptibility which is proportional to kT/δ for $kT \ll \delta$ in the orthogonal ensemble, and $(kT/\delta)^4$ in the

symplectic ensemble. Both the even and odd cases rapidly approach the Pauli expression as kT exceeds δ .

In comparing the above results with experiment, the effects of the particle size distribution must be taken into account. In describing the distribution of energy levels for a collection of small particles, with all of the particles taken to be spheres of the same size, the average level spacing δ has been introduced. The size enters only in determining this average level spacing δ which varies as a^{-3} . Thus the results must be folded into a particle size distribution. For a realistic size distribution the behavior for small a must be handled carefully because of the strong dependence of δ on a . For simplicity consider a "square" particle size distribution $P_s(a)$ centered at a_0 with width Δa . As an example of folding in the size distribution the average heat capacity $\langle C \rangle$ becomes

$$\langle C \rangle = \int C\left(\frac{kT}{\delta(a)}\right) P_s(a) da. \quad (46)$$

Expanding this in powers of $\Delta a/a_0$, one finds

$$\langle C \rangle \cong C\left(\frac{kT}{\delta_0}\right) + \left(\frac{\Delta a}{a_0}\right)^2 \left[\frac{kT}{4\delta_0} C'\left(\frac{kT}{\delta_0}\right) + \frac{3}{8} \left(\frac{kT}{\delta_0}\right)^2 C''\left(\frac{kT}{\delta_0}\right) \right], \quad (47)$$

where δ_0 is the level spacing for a particle of size a_0 . Therefore, in both the low- and high-temperature regions the particle size distribution modifies only the coefficient of the leading temperature-dependent term and not the form of the power-law dependence. Figure 11 shows the effect on the specific heat of folding in the particle size distribution, where we have considered the orthogonal

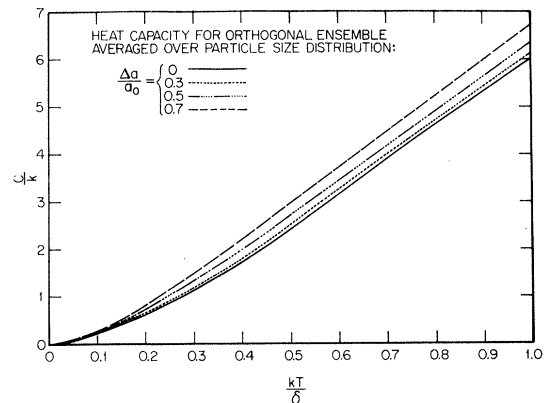


FIG. 11. Heat capacity after averaging over a square particle size distribution of width Δa . The initially unaveraged curve ($\Delta a/a_0 = 0$) is the heat capacity in the orthogonal ensemble, where a simple average of the even and odd cases has been taken.

case with $\Delta\alpha/a_0$ as large as 0.7. For lower values of $\Delta\alpha/a_0$ the specific heat is not greatly altered.

V. CONCLUDING REMARKS

We have focused our attention essentially on a detailed discussion of two problems connected with electrons in small metallic particles. The first problem was to show how discrete single-electron energy levels basically do affect the thermodynamics of small particles. Here, our "model specimen," described by equally spaced energy levels, proved to be the most suitable system to study the differences between the predictions of the canonical and grand canonical ensembles for finite particles. The second problem was considered in Sec. IV where we have developed for a collection of small particles a general approximation scheme in order to incorporate fully the effects of level statistics in the whole temperature range.

Experimental observation of small-particle effects could be used to test the fundamental assumptions made for both the thermal ensemble and the single-particle level distribution ensemble. Whereas even-odd effects have been suggested for the susceptibility^{15,16} no measurements of the electronic specific heat have been performed to our knowledge.¹⁷ Recently the preparation of probes containing small particles of definite size has been greatly improved¹⁸ which eventually may lead to more conclusive experiments.

Thermodynamic properties of superconducting particles with dimensions smaller than the coherence length may be studied experimentally more conveniently because of large fluctuations in a broad critical region. A simple theory which treats these fluctuations statically and includes equal level spacing has been worked out by us previously.¹⁹

Studying the behavior of isolated small particles should perhaps also be viewed as a first approximation in an understanding of the situation where there exists a coupling between the particles themselves or between particles and their surroundings. It seems that in normal-metal granules the interaction is mainly governed by the electrostatic activation energy of adding or removing an electron from a small particle, and this process does not reflect the level spacing of the isolated particles in an important manner. In superconducting grains, however, a Josephson-type coupling between particles leads to interesting consequences as was recently pointed out by Deutscher and Imry.²⁰ Several experiments have been reported within this context.^{21,22}

The properties of electrons in small metal particles in an electromagnetic field, and relaxation phenomena have been discussed by Kubo,^{3,23} Kawabata,²⁴ and Gor'kov and Eliashberg.¹⁰ The

latter authors claim that there should exist a large enhancement of the static dielectric constant caused by the finite level spacing. This phenomenon has been disputed experimentally,²⁵ although recently it has been indicated that small systems of interrupted metallic strands contained in certain compounds of platinum may exhibit the effect.²⁶

From a more fundamental point of view, dynamical processes in small particles are more difficult to treat than the static properties we have discussed in the present work. In thermodynamics we deal solely with energy levels, and the equal level system is a reasonable model which can be enlarged by employing the general fluctuation theory of spectra. In dynamical and relaxation processes we need additionally some ideas about the electron wave functions, matrix elements, and their dependence on statistical averages. Also, the surroundings of the small particle may play a more crucial role than for thermodynamic properties. Some further model calculations which include these features would be highly desirable.

ACKNOWLEDGMENT

One of the authors (B. M.) would like to thank the Department of Physics of the University of California in Santa Barbara for the hospitality offered to him.

APPENDIX

For the calculations of Sec. IV, a number of approximate formulas for the level-spacing distributions have been used. These approximate formulas will be discussed in this Appendix. The general spacing distribution is labeled by $P_{n-1}^{(\gamma)}(\alpha_1, \alpha_2, \dots, \alpha_n)$, where the label γ referring to the orthogonal, unitary, or symplectic ensembles, has the values 1, 2, and 4 in the respective formulas. The exact formulas for the nearest-neighbor distributions $P_0^{(\gamma)}(x)$ have been calculated previously.⁹ In Sec. II of the text we have given the small- x limit obtained for $P_0^{(\gamma)}(x)$. As mentioned, approximate formulas for the nearest-neighbor distributions have been calculated⁸ from Eq. (1) by specializing the equation to just two eigenvalues as described in Sec. II. This leads to the Wigner surmise $P_W(x)$ for the orthogonal ensemble. The results for the nearest-neighbor distributions are collected together in Table II, which lists the approximate formulas and the leading term from the exact formulas. For reference this table also includes the Poisson distribution. The spacing x is normalized with respect to its average value.

The coefficients of the leading small- x terms of the orthogonal ensemble and the Wigner surmise have a small relative difference of a few percent given by $(\frac{1}{6}\pi^2 - \frac{1}{2}\pi)/\frac{1}{6}\pi^2 = 4\frac{1}{2}\%$. In fact, over the entire range of x the approximate Wigner surmise

TABLE II. Nearest-neighbor distribution function for the different ensembles: approximate formulas and the leading terms in the exact formulas.

Ensemble (E)	Nearest-neighbor distribution $P_0^{(\gamma)}(x)$	
	Approximate formula	First term, exact formula
Orthogonal	$\frac{1}{2}\pi x \exp(-\frac{1}{4}\pi x^2)$	$\frac{1}{6}\pi^2 x$
Symplectic	$(\frac{8}{9})^6(x^4/\pi^3) \exp(-\frac{64}{9\pi^2}x^2)$	$\frac{32}{270}\pi^4 x^4$
Unitary	$(32/\pi^2)x^2 \exp(-4x^2/\pi)$	$\frac{1}{3}\pi^2 x^2$
Poisson		e^{-x}

and the exact formula $P_0^{(1)}(x)$ are in very good agreement.⁹ A similar close agreement for the other two ensembles is also indicated in the coefficients of the leading small- x terms. The leading term of the exact formulas has been used to calculate the leading low-temperature behavior of the specific heat and susceptibility found in Table I. However, in the interpolation scheme used to obtain results over the full temperature range, the approximate formulas in Table II were applied for the even case in the first-order approximation. At temperatures such that $kT/\delta \lesssim 0.1$, where the averaging is most important, this leads to errors of order a few percent. These small errors from the use of the approximate formulas decrease as one goes to the higher-order approximations, as discussed below.

The exact solution of a general spacing distribution $P_{n-1}^{(\gamma)}(x_1, x_2, \dots, x_n)$ is very difficult to calculate, since the limiting $N \rightarrow \infty$ behavior resulting from integrations taken over $W_N^{(\gamma)}$ [Eq. (1)] must be determined. Of the spacing distributions with more than one spacing variable, exact results are only available for $P_2^{(1)}(x_1, x_2)$. Mehta has presented a numerical tabulation of this function for a limited range of the variables.⁹ However, in Sec. IV of the present work one needs to integrate over these level-spacing distributions. For this purpose it is desirable to have reasonable approximations which are easier to handle. The approximation to the exact $P_{n-1}^{(\gamma)}(x_1, x_2, \dots, x_n)$ which we use is the generalization of the procedure which led to the approximate nearest-neighbor distributions. To obtain the approximate distribution of n spacings, Eq. (1) which gives the distribution of N ordered eigenvalues $W_N^{(\gamma)}(\epsilon_1, \dots, \epsilon_N)$ is specialized to the smallest number of levels needed to have n spacings; thus one uses $W_{n+1}^{(\gamma)}(\epsilon_1, \epsilon_2, \dots, \epsilon_{n+1})$. The variables of the $n+1$ successive levels are changed to n spacing variables given by $\Delta_i = \epsilon_{i+1} - \epsilon_i$, with the energy variable ϵ_1 remaining. This variable is then integrated over, to produce the spacing distributions from the eigenvalue distributions:

$$P_{n-1}^{(\gamma)}(\Delta_1, \dots, \Delta_n) \equiv \int_{-\infty}^{\infty} d\epsilon_1 W_{n+1}^{(\gamma)}(\epsilon_1, \Delta_1, \dots, \Delta_n). \quad (\text{A1})$$

The distribution $P_{n-1}^{(\gamma)}(\Delta_1, \Delta_2, \dots, \Delta_n)$ satisfies

$$\int_0^{\infty} d\Delta_1 \cdots \int_0^{\infty} d\Delta_n P_{n-1}^{(\gamma)}(\Delta_1, \dots, \Delta_n) = 1. \quad (\text{A2})$$

The Δ_i do not have the correct normalization at this point. The average values of the Δ_i here are generally different, while the average values for the exact spacing distributions are equal. This problem is resolved by scaling the variables Δ_i in terms of their average values,

$$\Delta_i - \Delta_i / \bar{\Delta}_i \equiv x_i, \quad (\text{A3})$$

which yields the properly normalized approximate distributions. In terms of the normalized spacing variables x_i , the distribution $P_{n-1}^{(\gamma)}(x_1, x_2, \dots, x_n)$ then satisfies

$$\bar{x}_i = \int_0^{\infty} dx_1 \cdots \int_0^{\infty} dx_n x_i P_{n-1}^{(\gamma)}(x_1, \dots, x_n) = 1 \quad (\text{A4})$$

with

$$\int_0^{\infty} dx_1 \cdots \int_0^{\infty} dx_n P_{n-1}^{(\gamma)}(x_1, \dots, x_n) = 1. \quad (\text{A5})$$

The calculation of some specific distributions by this method is described below.

For the calculation of $P_1^{(\gamma)}(x_1, x_2)$, one sets $n=3$ in Eq. (1), with spacings Δ_i defined as $\Delta_2 = \epsilon_3 - \epsilon_2$ and $\Delta_1 = \epsilon_2 - \epsilon_1$. Integrating over ϵ_1 from $-\infty$ to ∞ , one obtains the spacing distributions

$$P_1^{(\gamma)}(\Delta_1, \Delta_2) = C_3^{(\gamma)} (2\pi/3\gamma)^{1/2} [\Delta_1 \Delta_2 (\Delta_1 + \Delta_2)]^\gamma \times \exp[-\frac{1}{3}\gamma(\Delta_1^2 + \Delta_1 \Delta_2 + \Delta_2^2)]. \quad (\text{A6})$$

Similarly for the distributions with three spacings one finds

$$P_2^{(\gamma)}(\Delta_1, \Delta_2, \Delta_3) = C_4^{(\gamma)} (\pi/2\gamma)^{1/2} [\Delta_1 \Delta_2 \Delta_3 (\Delta_1 + \Delta_2)(\Delta_2 + \Delta_3)(\Delta_1 + \Delta_2 + \Delta_3)]^\gamma \times \exp[-\frac{1}{8}\gamma(3\Delta_1^2 + 4\Delta_2^2 + 3\Delta_3^2 + 4\Delta_1 \Delta_2 + 2\Delta_1 \Delta_3 + 4\Delta_2 \Delta_3)]. \quad (\text{A7})$$

The normalization coefficient $C_n^{(\gamma)}$ has been given before.⁸

Next the average values $\bar{\Delta}_i$ must be computed for the different ensembles in order to scale $\Delta_i \rightarrow \Delta_i / \bar{\Delta}_i \equiv x_i$. In general, this is difficult to do analytically,²⁷ but since the integration in Sec. IV must be done numerically, we have also resorted to the computer to find most of the average values. The values of $\bar{\Delta}_i$ for the two-spacing distributions, Eq. (A6), are found to be

$$\begin{aligned} \bar{\Delta}_1 = \bar{\Delta}_2 &= (27/4\pi)^{1/2} && \text{orthogonal,} \\ \bar{\Delta}_1 = \bar{\Delta}_2 &= 1.2853 && \text{symplectic,} \\ \bar{\Delta}_1 = \bar{\Delta}_2 &= 1.3464 && \text{unitary.} \end{aligned} \quad (\text{A8})$$

For the orthogonal three-spacing distributions one finds

$$\begin{aligned}\bar{\Delta}_1 = \bar{\Delta}_3 &= 0.9412, \\ \bar{\Delta}_2 &= 0.8399.\end{aligned}\quad (\text{A9})$$

Using these values according to the substitutions of (A3), one finally obtains the distributions $P_{n-1}^{(r)}(x_1, x_2, \dots, x_n)$ which fulfill Eq. (A4), and which were applied in Sec. IV.

The distributions are good approximations to the exact spacing distributions. One might suspect this since the simplest approximate distribution, the Wigner surmise, agrees closely with the exact nearest-neighbor distribution for the orthogonal ensemble $P_0^{(1)}(x)$. Some of the exact formulas have been tabulated elsewhere.^{9,28} To check our approximate distributions we have compared various moments such as $\langle x_1^2 \rangle$, $\langle x_1 x_2 \rangle$, etc., with results from exact numerical calculation. The agreement is good to within a few percent.

The more complicated formula, $P_2^{(1)}(x_1, x_2, x_3)$, has also been examined by another approach. If one were to consider calculating the exact $P_0^{(1)}(x)$, the first "symmetric" approximation past the Wigner surmise would be the function

$$\tilde{P}(x) = \int_0^\infty dx_1 \int_0^\infty dx_3 P_2^{(1)}(x_1, x_2, x_3). \quad (\text{A10})$$

For small x the first term of $\tilde{P}(x)$ goes as $\tilde{P}(x) = 1.625x$, while the exact solution goes as $P_0^{(1)}(x) = \frac{1}{6} \pi^2 x = 1.645x$. Thus the error is $\approx 1\%$, as com-

pared to the initial error of $\approx 4\frac{1}{2}\%$ for the Wigner surmise, indicating convergence of the approximate spacing formulas as the number of initial levels is increased.

This convergence is important in calculating the low-temperature behavior, where the averaging over spacings has the most effect. In Sec. IV it was stated that for the even case at low temperatures the general solution for the specific heat, Eq. (41), reduces to the simpler form Eq. (43) involving the exact spacing distribution. Now the exact spacing distributions are never used in the approximation scheme of Sec. IV, but nevertheless the errors are not large. In the first-order approximation of Eq. (44) at low temperatures, the exact $P_0^{(1)}(x)$ in Eq. (43) is replaced by the Wigner surmise $P_w(x)$. For this case the error of $4\frac{1}{2}\%$ is introduced into the coefficient multiplying the low-temperature behavior. In the third-order approximation at low temperatures only the first level in the partition function remains important similar to Eq. (43); however, due to the integration over the two spacings as in Eq. (A10), the spacing distribution in Eq. (43) is replaced by the distribution $\tilde{P}(x)$. But as we have noted, $\tilde{P}(x)$ differs from the exact $P_0^{(1)}(x)$ by an error of 1% in the low-temperature behavior. Thus the higher-order approximations converge rapidly to the exact low-temperature behavior given in Table I.

*This work formed part of a thesis submitted by R. Denton in partial fulfillment of the requirements for a Ph.D degree in Physics, University of California, Santa Barbara, Calif. 1971.

¹Research in Santa Barbara sponsored by the U.S. Air Force Office of Scientific Research, Air Force Systems Command, under Grant No. AFSOR-71-2007.

²National Science Foundation Senior Foreign Scientist, 1970-1971.

³A brief report on this work has been given previously; R. Denton, B. Mühlischlegel, and D. J. Scalapino, *Phys. Rev. Lett.* **26**, 707 (1971).

⁴R. Kubo, *J. Phys. Soc. Jap.* **17**, 975 (1962).

⁵R. Kubo, *Polarisation, Matière et Rayonnement, Livre de Jubilé l'honneur du Professeur A. Kastler* (Presses Universitaires de France, Paris, 1969).

⁶D. A. Greenwood, R. Brout, and J. A. Krumhansl, *Bull. Am. Phys. Soc.* **5**, 297 (1960).

⁷E. P. Wigner, *Proc. Camb. Philos. Soc.* **47**, 790 (1951).

⁸F. J. Dyson, *J. Math. Phys.* **3**, 140 (1962).

⁹M. L. Mehta, *Nucl. Phys.* **18**, 395 (1960).

¹⁰C. E. Porter and N. Rosenzweig, (*Ann. Acad. Sci. Fennicae AVI No. 44* (1960). See also C. E. Porter, *Statistical Theories of Spectra: Fluctuations* (Academic, New York, 1965). Many of the references in which the statistical-level distributions are studied can be found in this book of reprints. In addition, an excellent introductory chapter includes some of the formulas applied in this work.

¹¹M. L. Mehta, *Random Matrices and the Statistical Theory of Energy Levels* (Academic, New York, 1967).

¹²L. P. Gor'kov and G. M. Eliashberg, *Zh. Eksp. Teor. Fiz.* **48**, 1407 (1965) [*Sov. Phys.-JETP* **21**, 940 (1965)].

¹³E. T. Whittaker and G. N. Watson, *A Course of Modern*

Analysis (Cambridge U. P., London, 1935).

¹⁴S. Tomonaga, *Prog. Theor. Phys.* **5**, 544 (1950).

¹⁵H. Fröhlich, *Physica (Utr.)* **4**, 406 (1937). Fröhlich's small particles, however, are perfect cubes. Due to degeneracy, the electronic states near the Fermi level then have a much larger spacing given by $(P_F a)^2 \delta / \pi$.

¹⁶Note that $p_0(x) = P_0^{(1)}(x)$, but the remaining $p_n(x)$ are entirely distinct from the $P_n^{(r)}$ level distributions introduced in Sec. II.

¹⁷C. Taupin, *J. Phys. Chem. Solids* **28**, 41 (1967).

¹⁸S. Kobayashi, T. Takahashi, and W. Sasaki, *J. Phys. Soc. Jap.* **32**, 1234 (1972).

¹⁹Recently, an effect of size and surface on the specific heat of small lead particles was reported by V. Novotny, P. P. M. Meincke, and J. H. P. Watson [*Phys. Rev. Lett.* **28**, 901 (1972)]. However, these authors claim that they measure an enhanced lattice contribution. Whether or not their lead imbedded in a porous glass forms a system of well-isolated small particles is not clear to us.

²⁰E. Chok and H. Bömmel (private communication).

²¹B. Mühlischlegel, D. J. Scalapino, and R. Denton, *Phys. Rev. B* **6**, 1767 (1972).

²²G. Deutscher and Y. Imry (unpublished); G. Deutscher, *Phys. Lett. A* **35**, 28 (1971).

²³G. Deutscher, H. Fenichel, M. Gershenson, E. Grunbaum, and Z. Ovadiahu, in *Proceedings of the Thirteenth International Conference on Low Temperature Physics*, Boulder, 1972 (to be published).

²⁴P. Pellán, G. Dousselin, H. Cortes, and J. Rosenblatt, *Solid State Commun.* **11**, 427 (1972).

²⁵A. Kawabata and R. Kubo, *J. Phys. Soc. Jap.* **21**, 1765 (1966).

²⁴A. Kawabata, J. Phys. Soc. Jap. **29**, 902 (1970).

²⁵R. Dupree and M. A. Smithard, J. Phys. C **5**, 408 (1972).

²⁶M. J. Rice and J. Bernasconi, Phys. Rev. Lett. **29**, 113 (1972).

²⁷To our knowledge, of the two-spacing approximate

distributions only the orthogonal case has been calculated analytically; the result was given by Porter. See his book listed in Ref. 8.

²⁸P. B. Kahn, Nucl. Phys. **41**, 159 (1963).

PHYSICAL REVIEW B

VOLUME 7, NUMBER 8

15 APRIL 1973

Determination of the Surface Geometry for the Aluminum (110) and (111) Surfaces by Comparison of Low-Energy-Electron-Diffraction Calculations with Experiment

M. R. Martin and G. A. Somorjai

Inorganic Materials Research Division, Lawrence Berkeley Laboratory, and Department of Chemistry, University of California, Berkeley, California 94720

(Received 20 September 1972; revised manuscript received 6 November 1972)

Low-energy-electron-diffraction calculations have been extended to the (110) and (111) surfaces of aluminum in order to determine the spacing between the surface and bulk layers of the crystal. The Al(110) surface is found to be contracted by 10% to 15% from the bulk interlayer spacing, and the Al(111) surface is found to deviate from the bulk spacing by less than 5%. This amounts to a determination of the surface-layer position to within 0.1 Å. Results of calculations on all experimentally measured beams for these surfaces are compared with the experimental results for several assumed interlayer spacings. These comparisons are made with respect to qualitative peak shapes, peak positions, and relative peak amplitudes of the specular and all measured nonspecular beams from each surface. In order to achieve this agreement, it has been necessary to include the four outermost crystal layers and to describe the ion-core potential with five phase shifts in the 40–150-eV energy range.

I. INTRODUCTION

Encouraging progress has been made recently on the problem of crystal-surface-structure analysis by low-energy-electron diffraction (LEED). Several theoretical approaches to the multiple-scattering problem have led to the assembly of a variety of computer programs whose results have appeared recently in the literature. Multiple scattering has been taken into account by calculations based on a band-structure approach,^{1–3} a *t*-matrix approach,^{4–6} and the layer Korringa-Kohn-Rostoker (KKR) method.^{7,8} In addition, two perturbation methods have been proposed to reduce the computer-time requirements of the more exact methods.^{9–11}

In this paper we report on LEED calculations performed on several beams of the aluminum (110) and (111) surfaces. In Sec. II we describe the multiple-scattering method employed to construct the computer program. In Sec. III we discuss the parameters used throughout the calculations, and in Secs. IV and V we present the results of the aluminum (110) and (111) calculations, respectively, and compare them with experiment.

These calculations indicate that the position of the surface layer with respect to the bulk can be determined to within ~5% of the bulk interlayer spacing. The Al (110) surface layer is found to be located between 1.285 and 1.214 Å from the next-underlying layer which represents a contraction of

10–15% from the bulk interlayer spacing. The Al (111) surface-layer spacing is found to be equal to the bulk interplane spacing to within ~5%. In each case the surface-layer spacing is determined to within 0.1 Å.

II. DESCRIPTION OF CALCULATION

The computer program we have developed is based on the *t*-matrix approach to the multiple-scattering problem as formulated by Beeby,⁴ and extended by Duke and Tucker⁵ to include inelastic damping of the electron beam. The reader is referred to a paper by Laramore and Duke¹² in which the formalism that we employ in our calculation is set forth. Finite-temperature effects are accounted for in the Debye approximation, and the bulk lattice and surface layer can be assigned different Debye temperatures.

The scattering amplitude from a subplane λ , parallel to the surface, is proportional to a quantity $T_\lambda(\vec{k}_f, \vec{k}_i; E)$ [see Ref. 12, Eq. (3)], which is the *t*-matrix element for scattering from an incident plane wave whose wave vector is \vec{k}_i into an outgoing wave \vec{k}_f , at constant energy E . This quantity is expanded in an angular-momentum representation and one is concerned with evaluating a square matrix of dimension $(l+1)^2 \times (l+1)^2$, $T_\lambda^{LL'}$, where l is the angular-momentum quantum number corresponding to the highest-order phase shift $[\delta_l(E)]$ used to characterize the ion-core potential.

The evaluation of this matrix can be accomplished